

Signaling and Regulation

Long-term Stability of Demethylation after Transient Exposure to 5-Aza-2'-Deoxycytidine Correlates with Sustained RNA Polymerase II Occupancy

Jacob D. Kagey^{1,2}, Priya Kapoor-Vazirani^{2,3}, Michael T. McCabe^{2,3}, Doris R. Powell^{2,3}, and Paula M. Vertino^{1,2,3}

Abstract

DNA methyltransferase inhibitors are currently the standard of care for myelodysplastic syndrome and are in clinical trials for leukemias and solid tumors. However, the molecular basis underlying their activity remains poorly understood. Here, we studied the induction and long-term stability of gene reactivation at three methylated tumor suppressor loci in response to the DNA methyltransferase inhibitor 5-aza-2'-deoxycytidine (5-azaCdR) in human breast cancer cells. At the *TMS1/ASC* locus, treatment with 5-azaCdR resulted in partial DNA demethylation, the reengagement of RNA polymerase II (Pol II), and a shift from a repressive chromatin profile marked with H3K9me2 and H4K20me3 to an active profile enriched in H3ac and H3K4me2. Using a single-molecule approach coupling chromatin immunoprecipitation with bisulfite sequencing, we show that H3ac, H3K4me2, and Pol II selectively associated with the demethylated alleles, whereas H3K9me2 preferentially marked alleles resistant to demethylation. H4K20me3 was unaffected by DNA demethylation and associated with both unmethylated and methylated alleles. After drug removal, *TMS1* underwent partial remethylation, yet a subset of alleles remained stably demethylated for over 3 months. These alleles remained selectively associated with H3K4me2, H3ac, and Pol II and correlated with a sustained low level of gene expression. *TMS1* alleles reacquired H3K9me2 over time, and those alleles that became remethylated retained H3ac. In contrast, *CDH1* and *ESR1* were remethylated and completely silenced within ~1 week of drug removal, and failed to maintain stably unmethylated alleles. Our data suggest that the ability to maintain Pol II occupancy is a critical factor in the long-term stability of drug-induced CpG island demethylation. *Mol Cancer Res*; 8(7); 1048–59. ©2010 AACR.

Introduction

Cell type-specific gene expression patterns are established and maintained in part by epigenetic mechanisms including DNA methylation and posttranslational histone modifications. In mammals, DNA methylation occurs at cytosine residues found within the context of CpG dinucleotides, which are underrepresented in the genome but can be found in clusters called CpG islands that are associated with the regulatory regions of approximately 70% of human genes (1–3). In normal cells, most CpG islands are

unmethylated and transcriptionally competent. Methylation of CpG islands is associated with stable and heritable gene silencing (4). In addition to DNA methylation, posttranslational modifications of the histone tails contribute to epigenetic regulation. Unmethylated CpG islands tend to be packaged into nucleosomes marked with “active” histone modifications, including histone H3 acetylation of lysines 9 and 14 (H3ac) and histone H3 lysine 4 dimethylation and trimethylation (H3K4me2/3). Methylated CpG islands are generally depleted of these active marks and are alternatively marked by a subset of “repressive” histone modifications, including histone H3 lysine 9 dimethylation and trimethylation (H3K9me2/3) and histone H3 lysine 27 trimethylation (H3K27me3; refs. 5, 6).

Genome-wide epigenetic alterations occur in cancer. There is an overall hypomethylation of the genome concurrent with the aberrant hypermethylation of a subset of CpG islands (7). This aberrant methylation of CpG islands in cancer is accompanied by a shift from a permissive to a more repressive histone modification profile generally characterized by the loss of H3ac and H3K4me2/3 and the acquisition of H3K9me2/3 (8–10). Recent work suggests that the epigenetic silencing of some loci also involves a shift in histone H4 modifications, including loss of histone

Authors' Affiliations: ¹Graduate Program in Genetics and Molecular Biology, ²Department of Radiation Oncology, Emory University School of Medicine, and ³Winship Cancer Institute, Emory University, Atlanta, Georgia

Note: Supplementary data for this article are available at Molecular Cancer Research Online (<http://mcr.aacrjournals.org/>).

Current address for M.T. McCabe: Cancer Research, Oncology R&D, GlaxoSmithKline, 1250 South Collegeville Road, Collegeville, PA 19426.

Corresponding Author: Paula M. Vertino, Emory University, 1365-C Clifton Road Northeast, Room 4086, Atlanta, GA 30322. Phone: 404-778-3119; Fax: 404-778-5530. E-mail: pvertin@emory.edu

doi: 10.1158/1541-7786.MCR-10-0189

©2010 American Association for Cancer Research.

H4 acetylated at K16 (H4K16Ac) and gain of histone H4 trimethylated at lysine 20 (H4K20me₃; ref. 11). The combination of CpG island methylation and accompanying histone modifications is associated with stable gene repression and is one mechanism leading to the heritable inactivation of tumor suppressor genes during tumor progression (12, 13).

The finding that tumor suppressor genes are often inactivated by epigenetic means and that these events can play a direct role in cancer initiation and progression provides a compelling rationale for the use of inhibitors of DNA methyltransferases (DNMT) and histone-modifying enzymes as a therapeutic strategy (6, 14). Over the last decade, there has been considerable effort in the clinical development of DNMT and histone deacetylase (HDAC) inhibitors in cancer therapy. For example, 5-aza-2'-deoxycytidine (5-azaCdR; decitabine) and 5-aza-cytidine (Vidaza) have become the standard of care for myelodysplastic syndrome and have shown promise in the treatment of leukemias (6, 15). In these cases, DNMT inhibitors have shown both higher response rates and increased survival when compared with more traditional cytotoxic chemotherapeutic agents (14, 16). There is hope that such agents might also be useful in the treatment of solid tumors, if not as single agents then in combination with other epigenetic inhibitors (e.g., HDAC inhibitors) or as a strategy to sensitize cells to conventional chemotherapy (for example, see ref. 17).

Despite their clinical success, there is still much to understand about the molecular mechanisms underlying the clinical activity of these agents and the durability of response. Studies in cell culture have shown that 5-azaCdR treatment induces DNA demethylation and reactivation of epigenetically silenced tumor suppressor genes. This reactivation is accompanied by the loss of some repressive histone modifications (e.g., H3K9me₂) and the reappearance of active histone modifications (e.g., H3ac and H3K4me₂; refs. 18-20). However, the chromatin structure of CpG islands does not return to a fully active configuration due to the preservation of some repressive histone modifications unaffected by DNA demethylation such as H3K27me₃ and H3K9me₃, leaving open the potential for resiliencing after drug removal (20). Molecular analyses from biopsy-driven clinical trials indicate that global and gene-specific DNA demethylation is achievable *in vivo*. However, in cases where specific gene demethylation has been detected, remethylation is often observed within a few weeks of treatment (14).

To further understand the long-term effects of transient 5-azaCdR treatment on tumor suppressor gene reactivation, we studied the dynamics of DNA methylation, gene expression, and histone modifications at *TMS1/ASC* (target of methylation-induced silencing 1), a CpG island-associated proapoptotic gene that is frequently silenced in conjunction with DNA hypermethylation in human breast, prostate, and lung cancers (21). We find that 5-azaCdR-induced reactivation of *TMS1* is accompanied by DNA demethylation and a shift from a repressive histone profile

to a more active profile that includes the reassociation of RNA polymerase II (Pol II) with the *TMS1* promoter. Although a fraction of *TMS1* alleles are remethylated after drug removal, there is a subpopulation that remained stably unmethylated for at least 27 passages in culture (~3 months). This subpopulation is associated with both active (H3ac and H3K4me₂) and repressive histone marks (H4K20me₃) and remains selectively occupied by Pol II. Our data suggest that the ability to attain and to maintain Pol II occupancy is a critical factor in the long-term stability of DNA demethylation and gene expression after drug-induced reactivation.

Materials and Methods

Cell culture and 5-azaCdR treatments

MDA-MB231 cells were obtained from the American Type Culture Collection and cultured in DMEM supplemented with 10% fetal bovine serum and 2 mmol/L L-glutamine. For 5-azaCdR treatments, 5×10^4 MDA-MB231 cells were plated in a 10-cm dish 24 hours before treatment with 0.5 μ mol/L 5-azaCdR. Medium containing fresh 5-azaCdR was applied every other day for 6 days. Following treatment, cells were maintained in the absence of 5-azaCdR and split 1:10 every 3 days for 27 passages (~3 months). Cells were harvested and DNA, RNA, and chromatin were collected at 0, 3, 6, 9, and 27 passages after treatment.

Methylation-specific PCR

Genomic DNA (2 μ g) was bisulfite modified using the EZ DNA methylation kit (Zymo), and ~50 ng modified DNA used as template for methylation-specific PCR (MSP) as previously described (22). PCR conditions used were 5 minutes at 95°C, followed by 35 cycles of 30 seconds at 95°C, 45 seconds at 58°C, and 45 at 72°C, with a final 5-minute extension at 72°C. PCR products were resolved on a 1.5% agarose gel and stained with ethidium bromide. MSP primers are described in Supplementary Table S1.

Combined bisulfite restriction analysis

Bisulfite-modified DNA was amplified using primers devoid of any CpGs. Amplified products were purified with the PCR Purification kit (Qiagen), digested overnight at 37°C with either *Fnu4HI* or *XmnI*, precipitated, and resolved on a 2.0% agarose gel (23). Relative intensities of digested and undigested bands were quantified with ImageQuant 5.2, and percent methylation was determined as the combined intensity of the digested bands relative to that of all bands (undigested and digested). Primer sequences are in Supplementary Table S1.

Genomic bisulfite sequencing

Genomic bisulfite sequencing (GBS) was done as previously described (24). Briefly, bisulfite-modified DNA was amplified using primers devoid of CpGs as described above. PCR products were TA cloned (Invitrogen) and

transformed into chemically competent *Escherichia coli*, and plasmid DNA isolated from 10 to 17 individual colonies was sequenced. Bisulfite sequencing data were analyzed using the BiQ Analyzer software (25). Primer sequences are listed in Supplementary Table S1.

Reverse transcription-PCR

RNA was isolated using the RNeasy kit (Qiagen) and reverse transcribed with random hexamer primers and Moloney murine leukemia virus reverse transcriptase (24). Quantitative real-time PCR was used to analyze gene-specific transcripts, and their levels were normalized to 18S rRNA as previously described (11). Primer sequences are listed in Supplementary Table S1.

Chromatin immunoprecipitation and chromatin immunoprecipitation–bisulfite sequencing

Chromatin immunoprecipitation (ChIP) was done as previously reported (11). The following antibodies were used for specific immunoprecipitations: H3ac (Millipore), H3K4me2 (Millipore), H3K9me2 (Millipore), H4K20me3 (Abcam), and Pol II (Santa Cruz Biotechnology). Immunoprecipitated DNA was analyzed by quantitative PCR with primers for *TMS1*, *CDH1*, or *ESR1* (11). ChIP-bisulfite sequencing (ChIP-bis) was adapted from the ChIP-MSP protocol initially reported by Zinn et al. (26). Immunoprecipitated DNA from the ChIP procedure was subjected to bisulfite conversion as described above. Modified DNA was then amplified using *TMS1*-specific bisulfite sequencing primers listed in Supplementary Table S1. PCR products were purified and cloned, and plasmid DNA from individual colonies was sequenced.

Results

TMS1 is a proapoptotic tumor suppressor gene containing a promoter-associated CpG island that is frequently methylated and silenced in human cancers (Fig. 1A; ref. 21). Previously, we compared the epigenetic landscape of *TMS1* in breast cancer cell lines in which the *TMS1* gene is either unmethylated and the gene is expressed (MCF7) or methylated and silenced (MDA-MB231). We find that in MCF7 cells and other normal cell lines that express *TMS1* (e.g., IMR90), the CpG island is unmethylated, with DNase I hypersensitive sites, positioned nucleosomes, and distinct peaks of H4K16ac marking the boundaries between the unmethylated CpG island domain and surrounding methylated DNA (11, 27). In this state, the unmethylated CpG island is enriched for H3K4me2 and H3ac and depleted for H3K9me2. Conversely, MDA-MB231 cells have a densely methylated CpG island in which the CpG island–associated DNase I hypersensitive sites have been lost, nucleosomes are randomly positioned, and the active histone marks (H3K4me2, H4K16ac, and H3ac) have been replaced by repressive marks including H3K9me2 and H4K20me3. In this transcriptionally repressed state, H4K20me3 is local-

ized to a prominent peak just upstream of transcription start, whereas H3K9me2 is enriched throughout the CpG island (11).

Long-term effects of transient 5-azaCdR treatment at the *TMS1* locus

To investigate the long-term effects of a transient exposure to a DNA demethylating agent on the chromatin architecture at the *TMS1* locus, MDA-MB231 cells were treated with 0.5 $\mu\text{mol/L}$ of 5-azaCdR every other day for 6 days and then maintained in culture for 27 passages (~80 days) in the absence of 5-azaCdR. This protocol resulted in the inhibition of cell growth (1.8-fold decrease in doubling time over 6 days) but little DNA damage as determined by γH2Ax focus formation (data not shown). Consistent with previous work, treatment of MDA-MB231 cells with 5-azaCdR induced the reexpression of *TMS1* mRNA (Fig. 1B; ref. 24). However, whereas *TMS1* expression induced an average of 494-fold immediately following 5-azaCdR treatment, expression levels returned to ~3-fold over untreated cells within three passages after drug removal (Fig. 1B). This low level of *TMS1* expression was then maintained for at least 3 months (27 passages) in the absence of 5-azaCdR.

Treatment with 5-azaCdR resulted in an average demethylation of the *TMS1* CpG island from 100% methylated to 64% methylated as determined by combined bisulfite restriction analysis (COBRA) analysis (Fig. 1C). After the removal of 5-azaCdR, there was an initial burst of remethylation (from 64% to 76% methylation) after 3 passages, which leveled off at ~83% and was maintained at this level for 27 passages in culture in the absence of drug (Fig. 1D).

To distinguish between the possibilities that all *TMS1* alleles exhibit a partial remethylation or that distinct subpopulations of unmethylated and methylated alleles persist after the removal of 5-azaCdR, DNA was bisulfite modified and individual alleles were sequenced. Whereas all alleles were densely methylated in untreated MDA-MB231 cells, treatment with 5-azaCdR induced a heterogeneous methylation pattern consisting of alleles that were densely methylated, predominantly unmethylated, and those with a mixed pattern (Fig. 1D). Removal of 5-azaCdR resulted in the partial remethylation of the locus that, over time, resolved into two distinct subpopulations: one composed predominantly of methylated alleles and the other composed predominantly of unmethylated alleles (Fig. 1D). Interestingly, whereas there was a more checkered methylation profile seen in early post-5-azaCdR passages, the unmethylated alleles observed 27 passages later were almost entirely devoid of methylation.

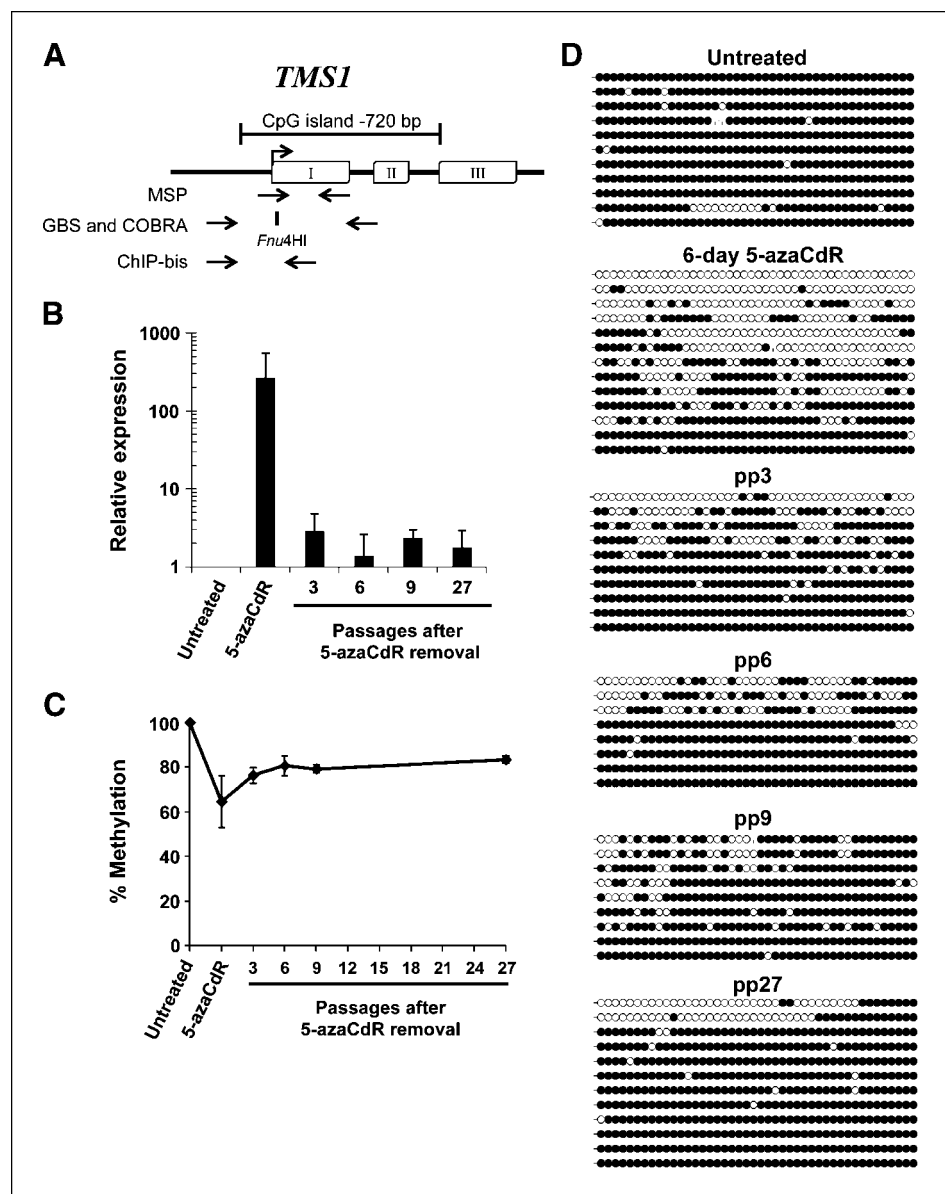
Effects of 5-azaCdR on the histone modifications at *TMS1*

To examine the effects of 5-azaCdR on chromatin at the *TMS1* locus, we used ChIP to map the histone modification profile before, immediately following, and over the course of 27 passages after treatment with 5-azaCdR. In

untreated MDA-MB231 cells, the *TMS1* locus was enriched for H3K9me2 and H4K20me3 (Fig. 2). Treatment with 5-azaCdR led to the accumulation of H3ac and H3K4me2, as well as a decrease in H3K9me2 at *TMS1* compared with untreated cells. This change was further accompanied by the reassociation of Pol II (Fig. 2). In contrast, the peak of H4K20me3, observed in untreated MDA-MB231 cells, was unaffected by 5-azaCdR. Additionally, H4K16Ac, which is found at the unmethylated *TMS1* locus in cells that express the gene (e.g., MCF7 cells; ref. 11), was not observed (data not shown). Thus, although 5-azaCdR treatment led to a shift to a more transcriptionally permissive chromatin configuration, it did not fully recapitulate the conformation observed in cells that normally express *TMS1*.

Over the course of 27 passages following the removal of 5-azaCdR, the enrichment of H3ac, H3K4me2, and Pol II was partially depleted at *TMS1* but still remained 3- to 21-fold higher than that of untreated MDA-MB231 cells (Fig. 2). H3K9me2 levels were partially restored over the same time frame but remained at levels lower than the untreated MDA-MB231 cells. This shift in the histone profile after the cessation of treatment coincided with the partial remethylation of DNA. The peak of H4K20me3 found upstream of the *TMS1* transcription start remained unchanged throughout the time course. Thus, although there was a partial return to the pretreatment chromatin state over time (DNA methylation and H3K9me2), a low level of active modifications and Pol II occupancy were maintained. Similar results were obtained from a second

FIGURE 1. *TMS1* expression and DNA methylation following the removal of 5-azaCdR. A, diagram of the *TMS1* gene. Open boxes, exons; arrow, transcription start site. The CpG island is indicated by the bracket. Primers used for MSP, GBS, and COBRA analyses are indicated below the gene, as is the position of the *Fnu4HI* restriction site used in COBRA analysis. B, *TMS1* mRNA abundance was measured immediately after treatment (5-azaCdR) or at the indicated time points after drug removal by quantitative reverse transcription-PCR and normalized to 18S rRNA. Shown is the fold change in expression relative to untreated cells from three independent time course experiments assayed in triplicate. Columns, mean; bars, SD. C, COBRA analysis of DNA methylation following the removal of 5-azaCdR at the *TMS1* locus. Points, mean percent methylation from three independent time course experiments; bars, SD. D, DNA methylation was analyzed by bisulfite sequencing at the indicated time points. Each line represents a single colony isolate (8-13 isolated per sample). pp, passages after 5-azaCdR treatment. Open circles, unmethylated CpG; filled circles, methylated CpG.



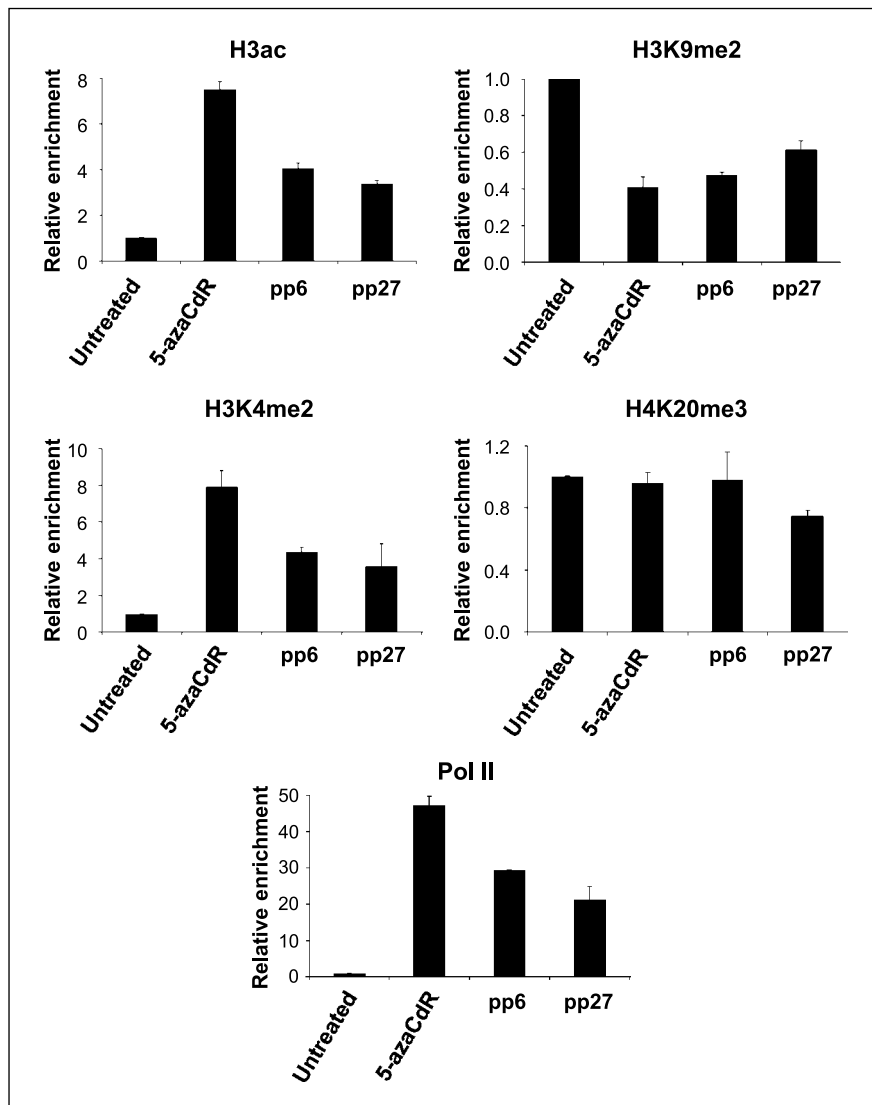


FIGURE 2. Histone modifications and RNA Pol II occupancy at *TMS1* after the removal of 5-azaCdR. MDA-MB231 cells were left untreated or treated with 0.5 $\mu\text{mol/L}$ 5-azaCdR for 6 d. Chromatin was isolated immediately after treatment (5-azaCdR) or at the indicated time after drug removal. Histone modifications and RNA Pol II occupancy were analyzed by ChIP followed by quantitative PCR. Percent enrichment was determined by comparison of immunoprecipitated DNA relative to input DNA at each time point using primer set 3 of the *TMS1* locus (11). Columns, mean of the fold change in enrichment relative to untreated MDA-MB231 cells from a single time course experiment assayed in triplicate; bars, SD. Similar results were obtained from a second independent time course (Supplementary Fig. S1).

independent time course (Supplementary Fig. S1) as well as at a second primer set (#5; ref. 11) in the *TMS1* CpG island (data not shown).

Coexisting methylated and demethylated *TMS1* alleles are packaged with differentially modified histones

Previous work has suggested that treatment with 5-azaCdR induces a “bivalent” chromatin signature at epigenetically reactivated tumor suppressor genes (20, 28), implying that both active (e.g., H3K4me2) and repressive (e.g., H3K27me3) modifications coexist on the same nucleosomes. Thus far, these studies have examined histone modifications at a population level within a mixed cell sample. We similarly show here that at a population level, both active and repressive epigenetic marks were present at the *TMS1* CpG island after treatment with 5-azaCdR. However, at the level of individual alleles, two distinct subpopulations with different DNA methylation patterns were observed.

To address the relationship between DNA methylation and histone modifications at the single-molecule level, we used a ChIP-bis approach in which the DNA component of chromatin immunoprecipitating with antibodies specific to Pol II or the various histone modifications was isolated, bisulfite modified, and analyzed for methylation status by sequencing of individual alleles. As a control, DNA isolated from fixed and sheared input chromatin in the absence of antibody was also analyzed. Consistent with naked DNA (Fig. 2C), DNA isolated from total chromatin directly after 5-azaCdR treatment showed a mixed DNA methylation pattern consisting of ~60% overall methylation (Fig. 3A). ChIP-bis showed that H3Ac, H3K4me2, and Pol II were selectively associated with the unmethylated alleles in this population, as indicated by the relative enrichment of unmethylated DNA (decreased methylation density) in the immunoprecipitated DNA relative to input chromatin (Fig. 3A). In contrast, H3K9me2 was selectively associated

with the methylated alleles immediately following treatment with 5-azaCdR (84% methylation density compared with 61% in input; Fig. 3B). The distribution of alleles associated with H4K20me3 had a methylation profile similar to that of input DNA (67% methylation density compared with 61%), suggesting that the nucleosomes marked by this modification associate with both methylated and unmethylated DNA, consistent with our observation that total levels of H4K20me3 at *TMS1* were unaltered by treatment with 5-azaCdR (Fig. 2). Overall, these data suggest that treatment with 5-azaCdR leads to the coordinated demethylation of DNA and loss of H3K9me2, and that the chromatin associated with these demethylated alleles was selectively marked by H3Ac and H3K4me2 and bound by Pol II.

To investigate the stability of the associated marks after the removal of 5-azaCdR, we next did ChIP-bis in cells 27 passages after drug removal. The DNA associated with total chromatin at this point had undergone a partial remethylation (from 61% to 79% methylation), similar to that observed for naked DNA analyzed by GBS (compare Figs. 1D and 3A). After 27 passages, H3K4me2-modified histones and Pol II remained predominantly associated with the unmethylated subpopulation of alleles (21% and 11% methylation density, respectively; Fig. 3B). However, H3Ac, which selectively associated with the unmethylated alleles immediately after treatment, was now associated with both methylated and unmethylated alleles (from 12% to 68% methylation density), suggesting that the presence of H3Ac does not prevent the remethylation of *TMS1* alleles. H3K9me2-marked histones, enriched on the methylated alleles immediately after treatment, were associated with both unmethylated and methylated *TMS1* alleles at a ratio that was similar to that of input chromatin (76% total methylation compared with 79%) and to that immediately following treatment. This, together with the data showing that *TMS1* alleles overall recover H3K9me2 over time (Fig. 2), indicates that alleles that become remethylated also reacquire H3K9me2 over time. H4K20me3, on the other hand, remained associated with both unmethylated and methylated alleles at a ratio similar to input both immediately after 5-azaCdR and 27 passages later. Thus, following the removal of 5-azaCdR in culture, we observe the preservation of a subset of unmethylated alleles uniquely marked by both active and repressive histone marks.

***ESR1* and *CDH1* are completely remethylated and silenced following transient exposure to 5-azaCdR**

A comparison of the data presented above with that of other single-gene studies examining the remethylation following 5-azaCdR treatment suggests that there may be gene-specific variations in the remethylation kinetics following the removal of 5-azaCdR (19, 20, 29). This may reflect intrinsic differences in their underlying epigenetic regulation or could be a consequence of differences between the cell lines and treatment protocols used in different studies. To address this question, we monitored two additional tumor suppressor genes, *CDH1* and *ESR1* (Figs. 4A and 5A), both of which are CpG island-

associated genes that are aberrantly methylated and silenced in human breast cancers and the MDA-MB231 cells used here (30). Like *TMS1*, the expression of *CDH1* and *ESR1* was substantially induced after 5-azaCdR treatment (Figs. 4B and 5B). In contrast to *TMS1*, which maintained a low yet stable expression level severalfold above untreated cells, both *CDH1* and *ESR1* were completely resiled within three passages (~9 days) after drug removal (Figs. 4B and 5B). Analysis of a single CpG site via COBRA analysis showed that *CDH1* and *ESR1* exhibited similar remethylation kinetics to *TMS1* (Figs. 1C, 4C, and 5C), in that all three genes were initially demethylated by 40% to 50% during treatment and then ultimately remethylated to 82% to 85%. However, a more detailed methylation analysis by GBS revealed distinctions in the patterns of their remethylation. After 27 passages in the absence of 5-azaCdR, both *CDH1* and *ESR1* exhibited more uniform patterns of methylation, in that nearly all alleles exhibited some level of remethylation (Figs. 4D and 5D). Unlike *TMS1*, neither locus retained a subset of predominantly unmethylated alleles after 5-azaCdR treatment.

We also examined alterations in the histone profiles at the *CDH1* and *ESR1* CpG islands throughout the 5-azaCdR time course. As observed at *TMS1*, 5-azaCdR-induced reactivation of *CDH1* and *ESR1* was associated with the accrual of H3ac, H3K4me2, the loss of H3K9me2, and the reestablishment of Pol II occupancy (Figs. 4E and 5E). H4K20me3 was not present at significant levels at either gene in untreated MDA-MB231 cells (data not shown; ref. 11) and was not further analyzed. Although 5-azaCdR treatment induced a similar set of epigenetic changes at all three genes, there were differences in the ability to maintain the induced histone profiles after drug removal. At *CDH1*, low levels of H3K4me2 and H3ac were maintained throughout the time course, whereas these marks were completely depleted from *ESR1* by 27 passages after 5-azaCdR removal (Figs. 4E and 5E). Somewhat surprisingly, Pol II was still present at both *CDH1* and *ESR1* six passages after drug removal despite the lack of detectable gene expression. Ultimately, however, both *CDH1* and *ESR1* exhibited a complete loss of Pol II occupancy between 6 and 27 passages after drug removal (Figs. 4E and 5E). These differences in maintained histone profile may reflect the subtle differences in the extent of remethylation of individual alleles observed in GBS (Figs. 4D and 5D). Similar results were observed in a second independent time course (Supplementary Figs. S3 and S4). Thus, although a similar subset of epigenetic alterations is induced by treatment with 5-azaCdR at *TMS1*, *CDH1*, and *ESR1*, complete DNA remethylation and the return to stable gene repression correlated with an inability to maintain Pol II occupancy after drug removal.

Discussion

Here, we establish that the degree and long-term stability of tumor suppressor gene reactivation induced by 5-azaCdR are locus specific and correlate with the ability

to attain and maintain Pol II promoter occupancy. Detailed analysis of the *TMS1/ASC* locus showed that transient exposure to 5-azaCdR induces DNA demethylation, depletion of H3K9me2, and the reacquisition of H3ac and H3K4me2. This allows for the reengagement of Pol II on the *TMS1* promoter and gene reactivation. Using a single-molecule approach, we show that these acquired active marks (H3ac, H3K4me2, and Pol II) preferentially associate with demethylated alleles, whereas H3K9me2 was selectively enriched on those alleles that remain methylated. H4K20me3, a mark typically associated with heterochromatin, was unaffected by 5-azaCdR treatment and was retained on both unmethylated and methylated alleles. After 3 months in the absence of drug, a subpopulation of unmethylated alleles persists and remains associated with the active marks and with Pol II, whereas *TMS1* alleles that remethylated lost both H3K4me2 and Pol II occupancy while maintaining H3ac. Thus, following the removal of 5-azaCdR, the *TMS1* CpG island is maintained in a unique epigenetic state, consisting of two distinct subpopulations of alleles, neither of which fully resembles the

repressed state in untreated MDA-MB231 cells, or that induced immediately after 5-azaCdR treatment.

Consistent with previous studies (8, 11, 26), we found that H3K9me2, H3K4me2, and DNA methylation status are tightly linked at the *TMS1* locus (as well as at *CDH1* and *ESR1*; refs. 18-20). Our single-molecule approach confirms that H3K9me2 is selectively depleted from the unmethylated alleles (i.e., it remains selectively associated with methylated alleles), suggesting that DNA methylation is necessary to maintain H3K9me2. Recent work shows that the histone methyltransferase G9a, thought to catalyze most H3K9me2 in euchromatin, interacts with components of the DNMT1 complex (31-33), suggesting a model in which DNA methylation and H3K9me2 may be coordinately maintained during DNA replication. Given that the incorporation of 5-azaCdR into DNA precipitates the degradation of DNMT1 (34), it is possible that the depletion of H3K9me2 is an indirect consequence of loss of DNMT1. After removal of 5-azaCdR, H3K9me2 remained predominantly associated with methylated alleles. Although we cannot distinguish between alleles that

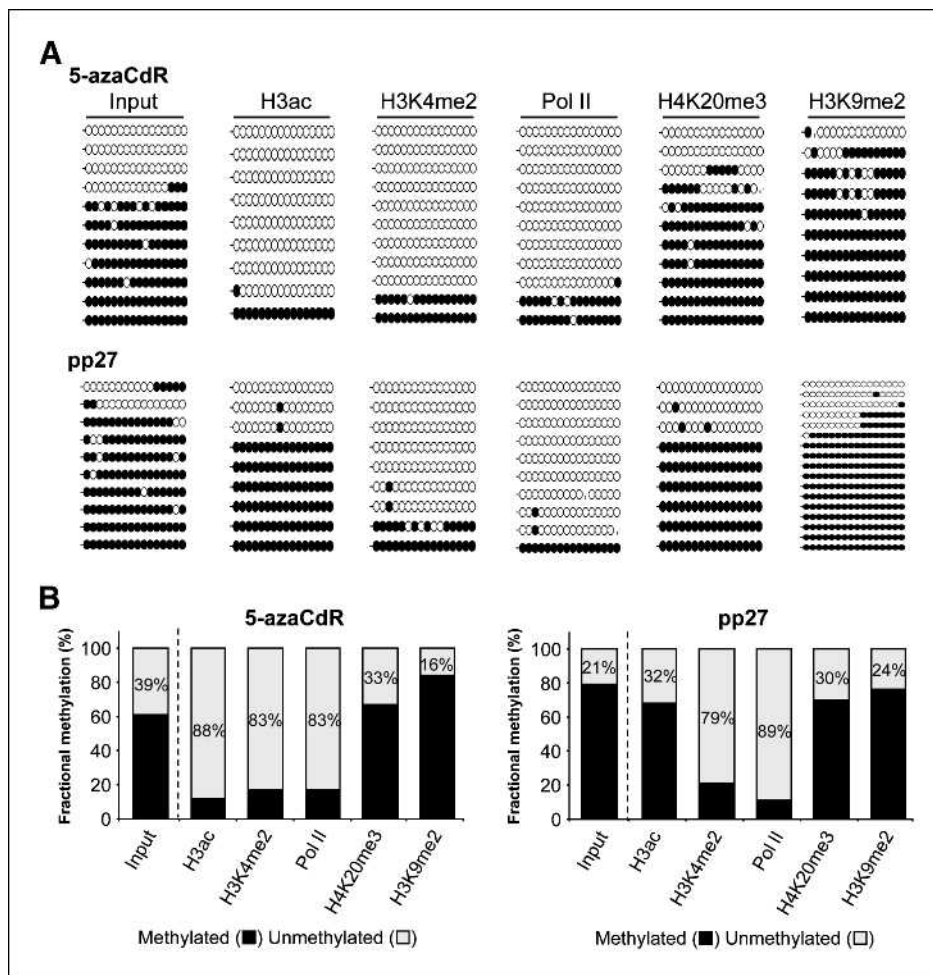


FIGURE 3. Single-molecule association between DNA methylation and chromatin modifications at the *TMS1* locus. MDA-MB231 cells were treated with 0.5 $\mu\text{mol/L}$ 5-azaCdR for 6 d. A, chromatin was isolated immediately after drug treatment (5-azaCdR) or 27 passages after drug removal (pp27) and immunoprecipitated with the indicated antibodies. Precipitated DNA was eluted, bisulfite modified, and amplified with the bisulfite sequencing primers indicated in Fig. 1A. For each immunoprecipitation, 9 to 17 individual clones were sequenced. Open circles, unmethylated CpGs; filled circles, methylated CpGs. Vertical hash marks represent missing data. B, overall methylation density was determined as the total number of methylated CpGs relative to total number of CpGs in all alleles analyzed.

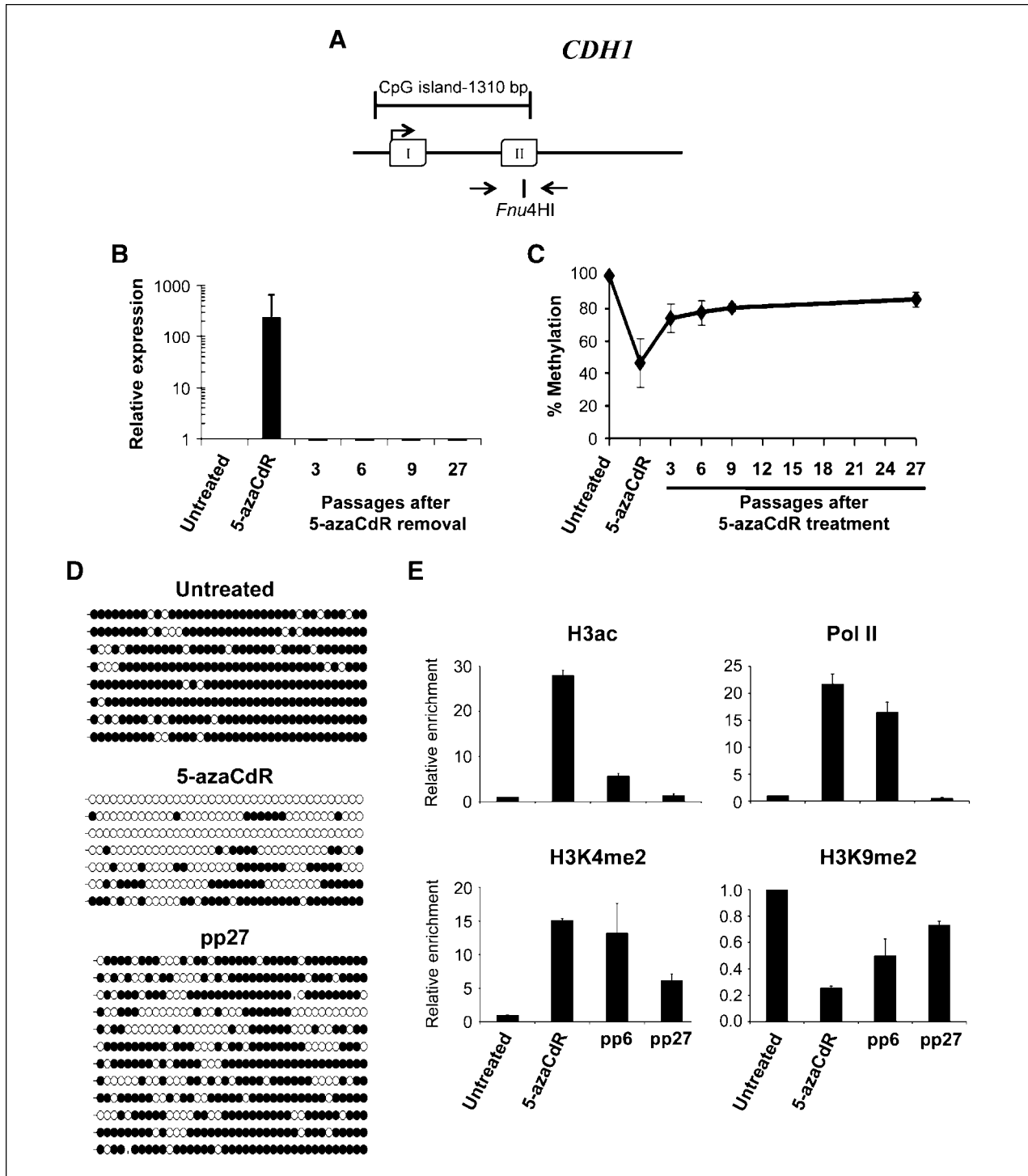


FIGURE 4. Analysis of *CDH1* during and following treatment with 5-azaCdR. A, diagram of *CDH1* CpG island. Open boxes, exons; arrow, transcription start site. The position of primers used for methylation analyses and the *Fnu4HI* restriction enzyme site used for COBRA analysis are indicated. B, *CDH1* mRNA expression was determined by quantitative reverse transcription-PCR and normalized to 18S rRNA. Shown is the fold change in expression relative to untreated cells from three independent experiments assayed in triplicate. Columns, mean; bars, SD. C, COBRA analysis of DNA methylation following the removal of 5-azaCdR at the *CDH1* locus. Points, mean percent methylation from three independent time course experiments; bars, SD. D, DNA methylation was further analyzed by bisulfite sequencing at the indicated time points. Each line represents a single colony isolate (8-11 isolated per sample). Open circles, unmethylated CpG; filled circles, methylated CpG. E, histone modifications and RNA Pol II occupancy were determined by ChIP as described in the legend to Fig. 2. Columns, mean of the fold change in enrichment relative to untreated MDA-MB231 cells from a single time course experiment assayed in triplicate; bars, SD. Similar results were obtained from a second independent time course (Supplementary Fig. S2).

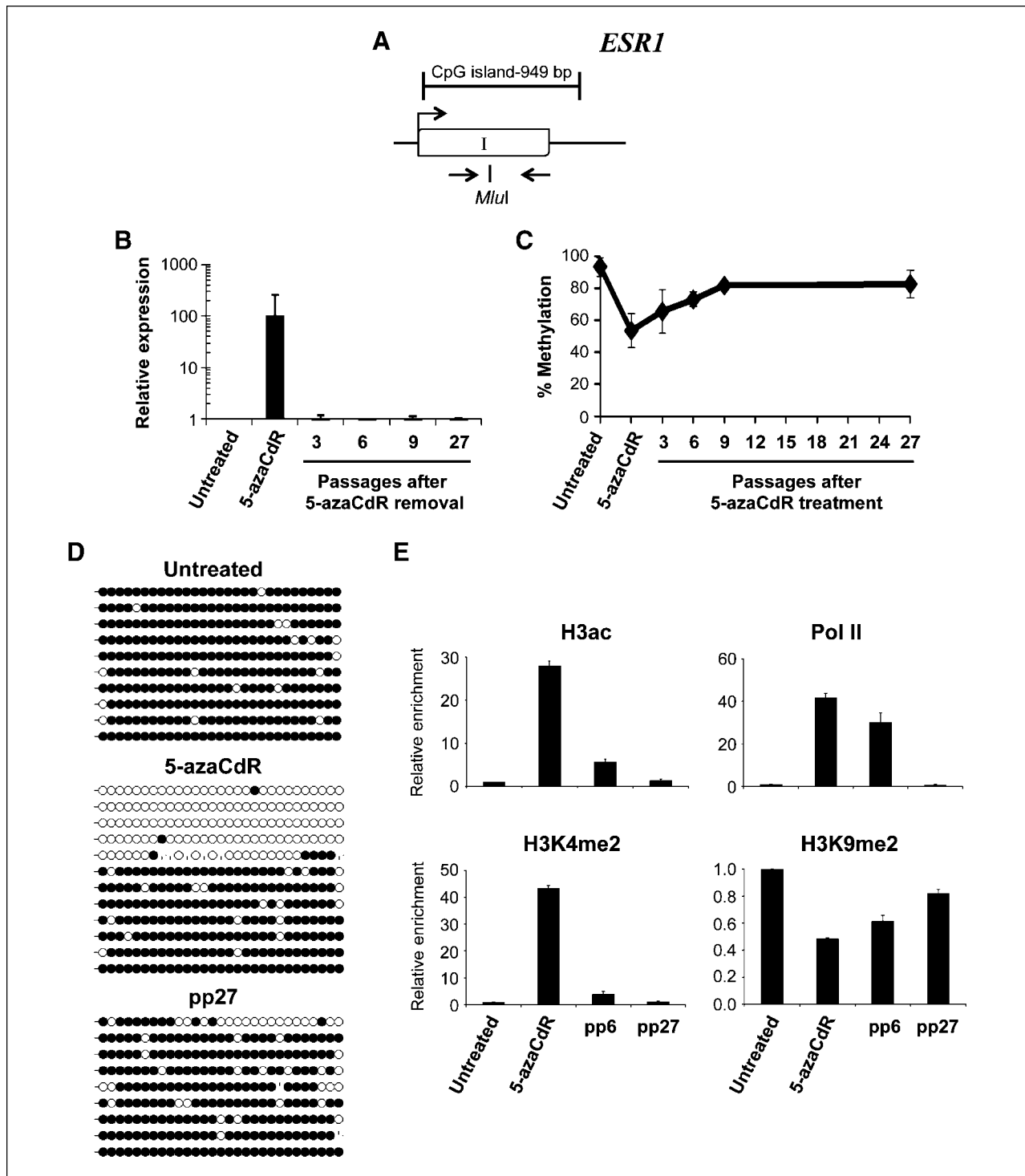


FIGURE 5. Analysis of *ESR1* during and following treatment with 5-azaCdR. A, diagram of *ESR1* CpG island. Open boxes, exons; arrow, transcription start site. The position of primers used for methylation analyses and the *MluI* restriction enzyme site used for COBRA analysis are indicated. B, mRNA expression was determined using primers specific to *ESR1*. Shown is the fold change in expression relative to untreated cells after internal normalization to 18S rRNA from three independent experiments assayed in triplicate. Columns, mean; bars, SD. C, COBRA analysis of DNA methylation at time points following the removal of 5-azaCdR at the *ESR1* locus as described in the legend to Fig. 1. D, DNA methylation was analyzed by bisulfite sequencing at the indicated time points. Each line represents a single colony isolate (9-12 isolated per sample). Open circles, unmethylated CpG; filled circles, methylated CpG; vertical dashes, missing data. E, histone modifications and RNA Pol II occupancy were determined by ChIP as described in the legend to Fig. 2. Columns, mean of the fold change in enrichment relative to untreated MDA-MB231 cells from a single time course experiment assayed in triplicate; bars, SD. Similar results were obtained from a second independent time course (Supplementary Fig. S3).

remethylated after drug removal from those that were never demethylated, these data together with the finding that H3K9me2 levels recover over time in parallel with DNA methylation (Fig. 2) suggest that alleles that remethylate also recover H3K9me2.

After the removal of 5-azaCdR, we find H3ac to be associated with both methylated and unmethylated *TMS1* alleles. Studies on the *hTERT* gene similarly found H3ac to associate with both methylated and unmethylated alleles (26). Our data suggest that drug-induced DNA demethylation is necessary to reestablish H3ac at *TMS1*, but once established, the presence of H3ac does not prevent the remethylation of DNA, nor does DNA remethylation drive the deacetylation of H3. Thus, although the combination of DNMT and HDAC inhibitors results in the synergistic reactivation of epigenetically silenced genes (35), they may have little effect on DNA remethylation and ultimately gene resiliencing after the cessation of treatment. Indeed, treatment with a HDAC inhibitor does not prevent the remethylation of the *p16* gene after 5-azaCdR-induced DNA demethylation (36).

Unlike many densely methylated genes reactivated by 5-azaCdR treatment that have a propensity to undergo remethylation and resiliencing after drug removal (18, 36), we found that a subset (~20%) of molecules is maintained in an unmethylated state at the *TMS1* locus for more than 80 days in culture in the absence of drug. These alleles were selectively occupied by RNA Pol II and marked by H3K4me2, and likely account for the residual low-level gene expression observed. In contrast, *ESR1* and *CDH1* were completely resilienced and all alleles remethylated over the same time frame. This raises the question of whether certain genes or genomic regions are differentially affected by 5-azaCdR treatment. Studies on the *MLH1* gene in colon cancer cells have similarly shown the maintenance of a stable subpopulation of unmethylated alleles (~7%) for at least 44 days after 5-azaCdR-induced reactivation (19). This study showed that 5-azaCdR-induced DNA demethylation was associated with the eviction of a single nucleosome near the transcription start site of *MLH1* and that the maintenance of this pattern of nucleosome depletion was both heritable and selective for the stably unmethylated subset of alleles (19). Although we did not examine nucleosome occupancy directly in this study, we have previously shown that the *TMS1* CpG island is spanned by positioned nucleosomes flanking a single nucleosome gap at the transcription start site in its unmethylated and actively transcribed state (11). We propose that this 5-azaCdR-induced nucleosome eviction allows for the reengagement of the Pol II complex with the demethylated promoter, perhaps filling the gap left behind by the evicted nucleosome, and it may be the maintenance of Pol II occupancy and/or the associated H3K4me2/3 deposition that prevent DNA remethylation. Consistent with this idea, recent studies examining histone methylation at 5-azaCdR-induced genes across the genome showed that reactivation of methylated genes was associated with accumulation of H3K4me2 distributed to either side of a char-

acteristic “dip” centered over transcription start (28). *CDH1* and *ESR1*, which exhibited total allelic remethylation, also failed to maintain significant Pol II occupancy after 5-azaCdR removal. The idea that Pol II occupancy may somehow protect CpG islands from *de novo* methylation is further supported by recent work showing that resistance of CpG islands to aberrant DNA methylation in cancer cells is better correlated with Pol II occupancy than gene expression on a genome-wide scale (37).

The fact that many genes seem to resilience to some extent after the removal of 5-azaCdR may be a direct result of the underlying chromatin structure. Whereas some repressive marks such as H3K9me2 are reversed by 5-azaCdR-induced demethylation, others (H3K9me3 and H3K27me3) are not affected and can be maintained in the absence of DNA methylation (20, 36). The persistence of such chromatin-mediated repression mechanisms may put the region at risk of remethylation after drug removal. We show here that H4K20me3 is similarly unaffected by alterations in DNA methylation and remains associated with both unmethylated and methylated *TMS1* alleles after the initial treatment with 5-azaCdR and throughout the course of DNA remethylation. These data suggest that there is a mechanism to maintain H4K20me3 at *TMS1* that is independent of DNA methylation. At present, the mechanisms targeting H4K20me3 to specific loci are unclear. Current models suggest that H4K20 methylation proceeds in a stepwise fashion, with PR-SET7 catalyzing monomethylation at this position, which is then acted on by SUV4-20H to catalyze dimethylation and trimethylation (38–41). Consistent with the idea that SUV4-20H is actively targeted to the *TMS1* locus in MDA-MB231 cells, we find that whereas an initial cotreatment with 5-azaCdR and transient knockdown of SUV4-20H lead to depletion of DNA methylation and H4K20me3, and synergistic reactivation of *TMS1* gene expression, it does not change the kinetics of *TMS1* resiliencing or remethylation after drug removal compared with 5-azaCdR alone (data not shown). Indeed, recent work from our lab suggests that whereas 5-azaCdR-mediated DNA demethylation allows for reassociation of Pol II with the locus, the residual presence of H4K20me3 inhibits Pol II elongation, resulting in the accumulation of initiated Pol II in the promoter-proximal region and downregulation of the full-length transcript.⁴ Whether this “enforcement” of RNA Pol II promoter-proximal pausing puts the gene at risk of subsequent remethylation remains to be determined.

The above considerations raise the question of whether the continued long-term inhibition of histone methyltransferases such as SUV4-20H might facilitate the maintenance of tumor suppressor gene activity after demethylation-induced reactivation. Thus far, our attempts to address this question have been hampered by the inability to create stable cell populations knocked down for SUV4-20H and the lack of inhibitors specific for this

⁴ P. Kapoor-Vazirani, et al., submitted for publication.

mark. Histone methyltransferase inhibitors have not yet been widely explored in cancer therapy, but several agents are beginning to emerge. Treatment of cancer cells with BIX01294, a small-molecule inhibitor with specificity for the G9a and GLP H3K9 methyltransferases, leads to a global and gene-specific depletion of H3K9me2 and reactivation of at least some genes (42). 3-Deazaneplanocin A (DzNEP) was originally reported to have selective effects on H3K27me3, which seem to be mediated through the destabilization of EZH2 and other PRC2 complex components (43). As an inhibitor of *S*-adenosylhomocysteine hydrolase, DzNEP might be expected to have indiscriminant effects on many *S*-adenosyl-L-methionine-dependent methyltransferases, and subsequent studies have shown that this agent has broad effects on the global levels of numerous histone methylation marks, including both active (e.g., H3K4me3 and H3K79me3) and repressive (e.g., H3K27me3, H3K9me2, and H3R2me2) modifications (44). Nevertheless, recent preclinical studies suggest that this agent may be particularly active in cancer types with a dependency on EZH2 (45). As such agents continue to be developed, future combination therapies and dosing schedules that incorporate both DNA methylation inhibitors and histone methyltransferase inhibitors will undoubtedly follow.

The DNMT inhibitors are now in widespread use for the treatment of myelodysplastic syndrome and are currently in clinical trials for acute myelogenous leukemia and other solid tumor types (15). Molecular analyses of bone marrow biopsies from patients treated with these agents have shown that global and gene-specific DNA demethylation is achievable *in vivo* (46, 47). The degree of demethylation varies between patients, and whether this is an important indicator of clinical response remains controversial and may depend on the compartment being analyzed (i.e., repetitive element methylation versus methylated tumor suppressor genes) or the surrogate marker measured (DNA methylation versus gene expression; refs. 14, 48). In most cases, a gradual return to pretreatment

methylation levels has been observed within a few weeks or by the start of the next treatment cycle (46, 48, 49). We show here that, at least in cell culture, the kinetics of DNA remethylation and gene silencing do not necessarily parallel each other and vary at different loci. Whereas *CDH1* and *ESR1* were resiled within a week after drug removal and before the complete remethylation of H3K9me2 and DNA, a subset of *TMS1* alleles remained stably unmethylated and occupied by Pol II for more than 3 months. The remethylation potential of a particular gene may be determined in part by the histone code present at that gene before demethylation and the persistence of certain histone methylation marks (e.g., H4K20me3). A thorough understanding of the underlying causes of these differences would be valuable in both developing new combined approaches incorporating inhibitors of other histone-modifying enzymes and improving existing epigenetic therapy regimens.

Disclosure of Potential Conflicts of Interest

No potential conflicts of interest were disclosed.

Acknowledgments

We thank Prity Patel, Harold Saavedra, and Arsene Adon for technical assistance and helpful discussions.

Grant Support

NIH grants 2RO1 CA077337 (P.M. Vertino), Department of Defense Congressionally Directed Medical Research Program Breast Cancer Program predoctoral fellowship W81XWH-08-1-0362 (J.D. Kagey), and American Cancer Society postdoctoral fellowship PF-07-130-01-MGO (M.T. McCabe). Paula Vertino is a Georgia Cancer Coalition Distinguished Cancer Scholar.

The costs of publication of this article were defrayed in part by the payment of page charges. This article must therefore be hereby marked *advertisement* in accordance with 18 U.S.C. Section 1734 solely to indicate this fact.

Received 05/01/2010; revised 05/27/2010; accepted 05/27/2010; published OnlineFirst 06/29/2010.

References

- Bird AP. CpG-rich islands and the function of DNA methylation. *Nature* 1986;321:209–13.
- McCabe MT, Brandes JC, Vertino PM. Cancer DNA methylation: molecular mechanisms and clinical implications. *Clin Cancer Res* 2009;15:3927–37.
- Lander ES, Linton LM, Birren B, et al. Initial sequencing and analysis of the human genome. *Nature* 2001;409:860–921.
- Baylin SB. DNA methylation and gene silencing in cancer. *Nat Clin Pract Oncol* 2005;2 Suppl 1:S4–11.
- Jenuwein T, Allis CD. Translating the histone code. *Science* 2001;293:1074–80.
- Egger G, Liang G, Aparicio A, Jones PA. Epigenetics in human disease and prospects for epigenetic therapy. *Nature* 2004;429:457–63.
- McCabe MT, Lee EK, Vertino PM. A multifactorial signature of DNA sequence and polycomb binding predicts aberrant CpG island methylation. *Cancer Res* 2009;69:282–91.
- Nguyen CT, Weisenberger DJ, Velicescu M, et al. Histone H3-lysine 9 methylation is associated with aberrant gene silencing in cancer cells and is rapidly reversed by 5-aza-2'-deoxycytidine. *Cancer Res* 2002;62:6456–61.
- Kondo Y, Shen L, Issa JP. Critical role of histone methylation in tumor suppressor gene silencing in colorectal cancer. *Mol Cell Biol* 2003;23:206–15.
- Fahrner JA, Eguchi S, Herman JG, Baylin SB. Dependence of histone modifications and gene expression on DNA hypermethylation in cancer. *Cancer Res* 2002;62:7213–8.
- Kapoor-Vazirani P, Kagey JD, Powell DR, Vertino PM. Role of hMOF-dependent histone H4 lysine 16 acetylation in the maintenance of TMS1/ASC gene activity. *Cancer Res* 2008;68:6810–21.
- Herman JG, Baylin SB. Gene silencing in cancer in association with promoter hypermethylation. *N Engl J Med* 2003;349:2042–54.
- Jones PA, Baylin SB. The fundamental role of epigenetic events in cancer. *Nat Rev Genet* 2002;3:415–28.
- Issa JP, Kantarjian HM. Targeting DNA methylation. *Clin Cancer Res* 2009;15:3938–46.

15. Oki Y, Aoki E, Issa JP. Decitabine—bedside to bench. *Crit Rev Oncol Hematol* 2007;61:140–52.
16. Silverman LR, Demakos EP, Peterson BL, et al. Randomized controlled trial of azacitidine in patients with the myelodysplastic syndrome: a study of the cancer and leukemia group B. *J Clin Oncol* 2002;20:2429–40.
17. Matei DE, Nephew KP. Epigenetic therapies for chemoresensitization of epithelial ovarian cancer. *Gynecol Oncol* 2010;116:195–201.
18. Coffee B, Zhang F, Ceman S, Warren ST, Reines D. Histone modifications depict an aberrantly heterochromatinized FMR1 gene in fragile X syndrome. *Am J Hum Genet* 2002;71:923–32.
19. Lin JC, Jeong S, Liang G, et al. Role of nucleosomal occupancy in the epigenetic silencing of the MLH1 CpG island. *Cancer Cell* 2007;12:432–44.
20. McGarvey KM, Fahrner JA, Greene E, Martens J, Jenuwein T, Baylin SB. Silenced tumor suppressor genes reactivated by DNA demethylation do not return to a fully euchromatic chromatin state. *Cancer Res* 2006;66:3541–9.
21. McConnell BB, Vertino PM. TMS1/ASC: the cancer connection. *Apoptosis* 2004;9:5–18.
22. Herman JG, Graff JR, Myohanen S, Nelkin BD, Baylin SB. Methylation-specific PCR: a novel PCR assay for methylation status of CpG islands. *Proc Natl Acad Sci U S A* 1996;93:9821–6.
23. Xiong Z, Laird PW. COBRA: a sensitive and quantitative DNA methylation assay. *Nucleic Acids Res* 1997;25:2532–4.
24. Levine JJ, Stimson-Crider KM, Vertino PM. Effects of methylation on expression of TMS1/ASC in human breast cancer cells. *Oncogene* 2003;22:3475–88.
25. Bock C, Reither S, Mikeska T, Paulsen M, Walter J, Lengauer T. BiQ Analyzer: visualization and quality control for DNA methylation data from bisulfite sequencing. *Bioinformatics* 2005;21:4067–8.
26. Zinn RL, Pruitt K, Eguchi S, Baylin SB, Herman JG. hTERT is expressed in cancer cell lines despite promoter DNA methylation by preservation of unmethylated DNA and active chromatin around the transcription start site. *Cancer Res* 2007;67:194–201.
27. Stimson KM, Vertino PM. Methylation-mediated silencing of TMS1/ASC is accompanied by histone hypoacetylation and CpG island-localized changes in chromatin architecture. *J Biol Chem* 2002;277:4951–8.
28. McGarvey KM, Van Neste L, Cope L, et al. Defining a chromatin pattern that characterizes DNA-hypermethylated genes in colon cancer cells. *Cancer Res* 2008;68:5753–9.
29. Coffee B, Zhang F, Warren ST, Reines D. Acetylated histones are associated with FMR1 in normal but not fragile X-syndrome cells. *Nat Genet* 1999;22:98–101.
30. Nass SJ, Herman JG, Gabrielson E, et al. Aberrant methylation of the estrogen receptor and E-cadherin 5' CpG islands increases with malignant progression in human breast cancer. *Cancer Res* 2000;60:4346–8.
31. Kim JK, Esteve PO, Jacobsen SE, Pradhan S. UHRF1 binds G9a and participates in p21 transcriptional regulation in mammalian cells. *Nucleic Acids Res* 2009;37:493–505.
32. Esteve PO, Chin HG, Smallwood A, et al. Direct interaction between DNMT1 and G9a coordinates DNA and histone methylation during replication. *Genes Dev* 2006;20:3089–103.
33. Dong KB, Maksakova IA, Mohn F, et al. DNA methylation in ES cells requires the lysine methyltransferase G9a but not its catalytic activity. *EMBO J* 2008;27:2691–701.
34. Ghoshal K, Datta J, Majumder S, et al. 5-Aza-deoxycytidine induces selective degradation of DNA methyltransferase 1 by a proteasomal pathway that requires the KEN box, bromo-adjacent homology domain, and nuclear localization signal. *Mol Cell Biol* 2005;25:4727–41.
35. Cameron EE, Bachman KE, Myohanen S, Herman JG, Baylin SB. Synergy of demethylation and histone deacetylase inhibition in the re-expression of genes silenced in cancer. *Nat Genet* 1999;21:103–7.
36. Egger G, Aparicio AM, Escobar SG, Jones PA. Inhibition of histone deacetylation does not block resiliencing of p16 after 5-aza-2'-deoxycytidine treatment. *Cancer Res* 2007;67:346–53.
37. Takeshima H, Yamashita S, Shimazu T, Niwa T, Ushijima T. The presence of RNA polymerase II, active or stalled, predicts epigenetic fate of promoter CpG islands. *Genome Res* 2009;19:1974–82.
38. Yang H, Mizzen CA. The multiple facets of histone H4-lysine 20 methylation. *Biochem Cell Biol* 2009;87:151–61.
39. Pannetier M, Julien E, Schotta G, et al. PR-SET7 and SUV4-20H regulate H4 lysine-20 methylation at imprinting control regions in the mouse. *EMBO Rep* 2008;9:998–1005.
40. Oda H, Okamoto I, Murphy N, et al. Monomethylation of histone H4-lysine 20 is involved in chromosome structure and stability and is essential for mouse development. *Mol Cell Biol* 2009;29:2278–95.
41. Schotta G, Sengupta R, Kubicek S, et al. A chromatin-wide transition to H4K20 monomethylation impairs genome integrity and programmed DNA rearrangements in the mouse. *Genes Dev* 2008;22:2048–61.
42. Ferro MT, Steegman JL, Escobedo L, et al. Ph-positive chronic myeloid leukemia with t(8;21)(q22;q22) in blastic crisis. *Cancer Genet Cytogenet* 1992;58:96–9.
43. Tan J, Yang X, Zhuang L, et al. Pharmacologic disruption of Polycomb-repressive complex 2-mediated gene repression selectively induces apoptosis in cancer cells. *Genes Dev* 2007;21:1050–63.
44. Miranda TB, Cortez CC, Yoo CB, et al. DZNep is a global histone methylation inhibitor that reactivates developmental genes not silenced by DNA methylation. *Mol Cancer Ther* 2009;8:1579–88.
45. Puppe J, Drost R, Liu X, et al. BRCA1-deficient mammary tumor cells are dependent on EZH2 expression and sensitive to Polycomb Repressive Complex 2-inhibitor 3-deazaneplanocin A. *Breast Cancer Res* 2009;11:R63.
46. Mund C, Hackanson B, Stresemann C, Lubbert M, Lyko F. Characterization of DNA demethylation effects induced by 5-aza-2'-deoxycytidine in patients with myelodysplastic syndrome. *Cancer Res* 2005;65:7086–90.
47. Gore SD, Baylin S, Sugar E, et al. Combined DNA methyltransferase and histone deacetylase inhibition in the treatment of myeloid neoplasms. *Cancer Res* 2006;66:6361–9.
48. Fandy TE, Herman JG, Kerns P, et al. Early epigenetic changes and DNA damage do not predict clinical response in an overlapping schedule of 5-azacytidine and entinostat in patients with myeloid malignancies. *Blood* 2009;114:2764–73.
49. Braiteh F, Soriano AO, Garcia-Manero G, et al. Phase I study of epigenetic modulation with 5-azacytidine and valproic acid in patients with advanced cancers. *Clin Cancer Res* 2008;14:6296–301.

Molecular Cancer Research

Long-term Stability of Demethylation after Transient Exposure to 5-Aza-2'-Deoxycytidine Correlates with Sustained RNA Polymerase II Occupancy

Jacob D. Kagey, Priya Kapoor-Vazirani, Michael T. McCabe, et al.

Mol Cancer Res 2010;8:1048-1059. Published OnlineFirst June 29, 2010.

Updated version Access the most recent version of this article at:
[doi:10.1158/1541-7786.MCR-10-0189](https://doi.org/10.1158/1541-7786.MCR-10-0189)

Supplementary Material Access the most recent supplemental material at:
<http://mcr.aacrjournals.org/content/suppl/2010/09/10/1541-7786.MCR-10-0189.DC1>

Cited articles This article cites 49 articles, 27 of which you can access for free at:
<http://mcr.aacrjournals.org/content/8/7/1048.full#ref-list-1>

Citing articles This article has been cited by 9 HighWire-hosted articles. Access the articles at:
<http://mcr.aacrjournals.org/content/8/7/1048.full#related-urls>

E-mail alerts [Sign up to receive free email-alerts](#) related to this article or journal.

Reprints and Subscriptions To order reprints of this article or to subscribe to the journal, contact the AACR Publications Department at pubs@aacr.org.

Permissions To request permission to re-use all or part of this article, use this link
<http://mcr.aacrjournals.org/content/8/7/1048>.
Click on "Request Permissions" which will take you to the Copyright Clearance Center's (CCC) Rightslink site.